www.sensorsportal.com

Sensors & Transducers

http://www.sensorsportal.com

Thermal Stability of Magnetic Compass Sensor for High Accuracy Positioning Applications

[1] Van-Tang PHAM, [2] Dinh-Chinh NGUYEN, [3] Quang-Huy TRAN, [2] Duc-Trinh CHU and [2] Duc-Tan TRAN

[1] VNU University of Science, Hanoi, Vietnam
[2] VNU University of Engineering and Technology, Hanoi, Vietnam
[3] Hanoi Pedagogical University No. 2, Vinhphuc, Vietnam
[1] Tel.: + 844.37547709, fax: + 844.37549338
[1] E-mail: tantd@vnu.edu.vn

Received: 16 September 2015 /Accepted: 30 November 2015 /Published: 30 December 2015

Abstract: Using magnetic compass sensors in angle measurements have a wide area of application such as positioning, robot, landslide, etc. However, one of the most phenomenal that affects to the accuracy of the magnetic compass sensor is the temperature. This paper presents two thermal stability schemes for improving performance of a magnetic compass sensor. The first scheme uses the feedforward structure to adjust the angle output of the compass sensor adapt to the variation of the temperature. The second scheme increases both the temperature working range and steady error performance of the sensor. In this scheme, we try to keep the temperature of the sensor is stable at the certain value (e.g. 25 ºC) by using a PID (proportional-integral-derivative) controller and a heating/cooling generator. Many experiment scenarios have implemented to confirm the effectivity of these solutions. *Copyright © 2015 IFSA Publishing, S. L.*

Keywords: Temperature, Stability, Feedback, Feedforward, Compass Sensor.

1. Introduction

Recently, magnetic compass sensors, along with several sensors or devices such as a gyroscope, accelerometer, inertial measurement unit (i.e. Integration of gyroscopes and accelerometer), Global Positioning System (GPS)... are must have devices that any moving objects are being equipped [1-5]. The stability of magnetic compass sensors is better than other fluxgate ones. Some disadvantages of this kind of sensor related to magnetic properties can be eliminated by the careful setting. However, the temperature effect cannot be neglected [6], especially in harsh conditions. There are two characteristics of temperature to consider: the sensitivity of the temperature coefficient and the offset drift with temperature. The sensitivity temperature coefficient will appear as a change in output gain of the sensor over temperature. The magnetic sensor offset drift with temperature causes drift. This will have a direct influence on the attitude and causes appreciable errors [7]. However, it is still a lack of a radical solution to overcome this limitation.

In this paper, we firstly investigate the influence of temperature to the accuracy of magnetic compass sensor output and the navigation system. Secondly, several signal processing algorithms are applied to cancel the sensor temperature offset drift, and the DC offset voltage as well as the amplifier offset voltage and its temperature drift. Lastly, two schemes of compensation are proposed to correct the angle provided by the compass sensor under the change of temperature. The first scheme adjusts the angle output due to the variance of the temperature and the second scheme tries to keep the temperature of the sensor is stable at the certain value (e.g. 25 ºC). The approach in the Scheme 1 is closed to most of conventional methods proposed to solve the temperature stability. The approach in the Scheme 2 is novel and potential to apply in real applications. Many experiment scenarios have implemented to evaluate these solutions.

2. Working Principles

2.1. Heading Determination Using the Earth's Magnetic Field

The Earth's magnetic field intensity is about 0.5 to 0.6 Gauss, and can be approximated to the dipole model. The magnetic poles do not coincide with the geographical poles, which are defined by the Earth's axis of rotation. The angle between the magnetic and the rotation axis is about 11.5° [8]. As we can see in Fig. 1, the magnetic field lines do not exactly point to geographic or the "true" north. Although the Earth's magnetic field is not perfectly uniform, the entire surface of the Earth is covered by a magnetic field which is suitable and sufficient enough to determine the direction.

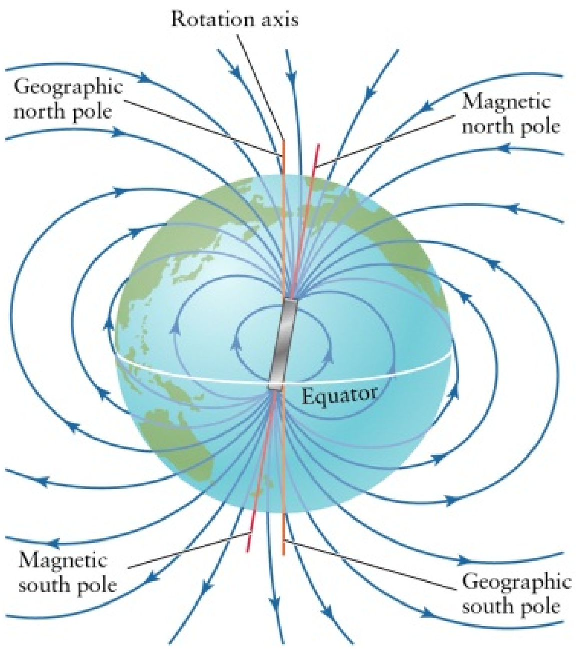

Fig. 1. Illustration of the Earth's magnetic field.

The Earth's magnetic field in a Cartesian coordinates system is shown in Fig. 2 [9]. In this figure, H_{eh} is the horizontal field component. The angle between the true north and the magnetic north is the declination λ. The angle between the magnetic field H_e and the horizontal plane is the inclination δ. The angle between the magnetic north and the x-axis of the compass sensor is the azimuth (or the heading) α.

The azimuth α can be calculated by

$$\alpha = \begin{cases} \arctan\left(H_{ey}/H_{ex}\right), & H_{ex} \neq 0 \\ \pi/2, & \left(H_{ey} > 0, H_x = 0\right) \\ -\pi/2, & \left(H_{ey} < 0, H_x = 0\right) \end{cases} \quad (1)$$

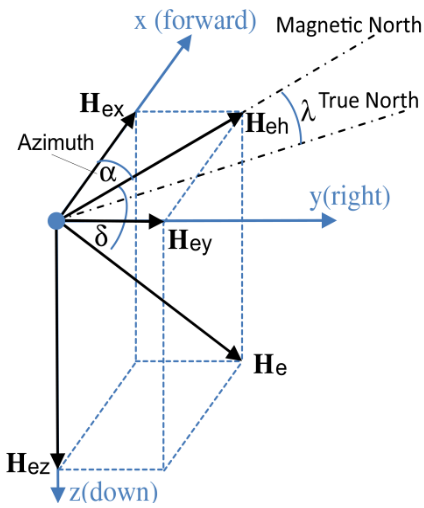

Fig. 2. Earth's magnetic field vector 0.

2.2. Magnetic Compass Sensor

Up to now, the magnetic field sensors have been still a primary means of navigation systems. Anisotropic Magnetoresistive (AMR) sensors have a simple fabrication process regarding the number of layers and materials used. Compared to other magnetometers, AMR sensors are also the most stable magnetoresistive sensor in term of bias and sensitivity. With the advancement of MEMS technology, triple axes of this type of sensor are available in a tiny package. Therefore, AMR sensors are still mostly used for low-cost inertial navigation systems [10].

The ARM effect was discovered in 1857 by William Thomson. In the AMR effect, the resistance of ferromagnetic alloys (alloy of Fe and Ni) is a function of the angle φ, between the magnetization and current (Fig. 3) [11]:

$$R = R_0 + \Delta R \cos^2 \varphi, \quad (2)$$

where $R_0 = R_{min}$, and $\Delta R = R_{max} - R_{min}$. The linearity of the equation and corresponding sensitivity is maximum if $\varphi = 45^o$.

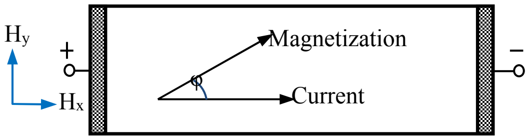

Fig. 3. Formation of φ in AMR sensor.

To compensate for the non-linear characteristics, "barber pole" structures have been introduced. The permalloy strip is covered with aluminum stripes oriented at 45° to the long axis of the strip (Fig. 4). The effect of the barber pole is to rotate the current direction by 45°, effectively changing the angle between the magnetization and the electrical current from α to (α-45°). The dependence of resistance now is linear around the null point.

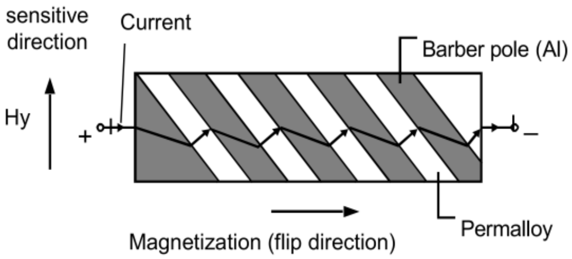

Fig. 4. Barber poles.

After linearization, R is shown

$$R = R_0 \pm \Delta R \frac{H_y}{H_0}, \tag{3}$$

where H_y is the measured magnetic field, and H_0 is the total anisotropy magnetic field.

AMR sensors are usually used in a Wheatstone bridge configuration with diagonally opposite sensors having barber pole orientations of ±45°. This arrangement helps reduce the temperature drift and increase the sensitivity of the sensor.

2.3. Temperature Stability for Magnetic Compass Sensor

The temperature effect is one of the important factors that greatly influence on the accuracy of the magnetic sensor. Thus, the temperature stability is a very important issue. Two basic temperature parameters are usually concerned: temperature dependence of sensitivity and the drift of the offset. Temperature dependence of sensitivity usually has simple sources such as temperature changes in permeability, resistivity, coil and core dimensions. There are many methods to compensate for temperature effect of AMR sensors. For example, a method to compensate for the drift of the offset is to use the flipping technique (Fig. 5). This technique cancels the drift of the offset, and the DC offset voltage as well as the amplifier offset voltage and its temperature drift. In the following section, the schemes are proposed to reduce the temperature dependence of sensitivity.

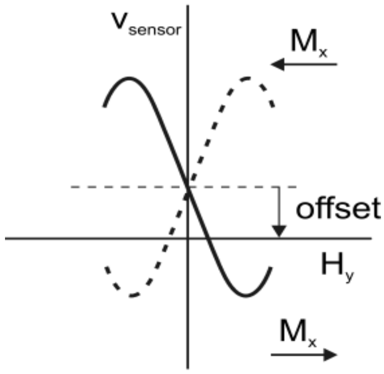

Fig. 5. The AMR sensor output after flipping of both polarities.

3. Design and Implementation the Temperature Compensation System

3.1. Feed-forward Compensation

The principle of this method is that a feed-forward structure is applied to compensate the error values of compass system (Fig. 6). A microcontroller is used to get the output values of both the compass and temperature sensors, and then it correct the output values of the compass sensor due to the variance of the temperature. In detail, from the experimental investigation, the compass sensor offers the highest accuracy at the room temperature (i.e. 25 °C). Thus, at an instance, the microprocessor computes the variance of instance temperature with 25 °C. This variance is then used to compute the compensated of the angle acquired from the compass sensor. This procedure is shown in Fig. 7.

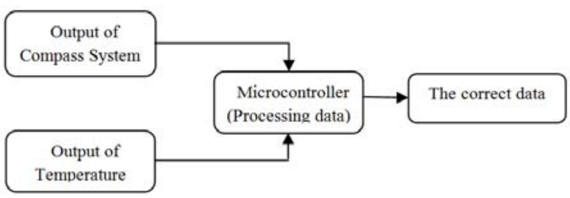

Fig. 6. Block diagram of the software compensated compass system.

The compass system used in this research is a CMPS03 compass sensor [13]. In the concerned temperature range from 18 °C to 53 °C, CMPS03 sensor is assumed to offer a linear relationship between the temperature variance and the sensor's sensitivity. According to the experiment, the sensitivity factor is 0.105 degrees per 1° Celsius.

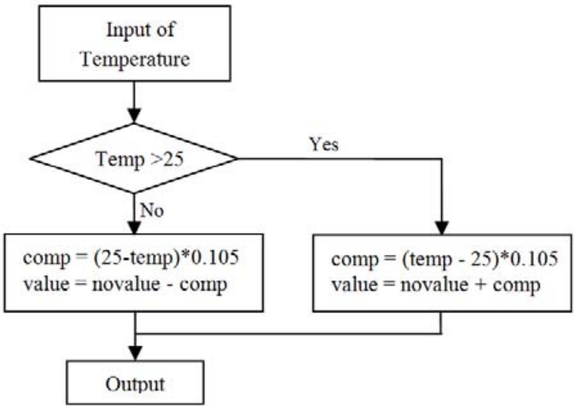

Fig. 7. Algorithm scheme of feed-forward compensation.

3.2. Feed-back Compensation

In order to overcome the limitation of the assumption of linearity, the feedback structure is proposed in this section (see Fig. 8). In this scheme, we try to keep the working temperature of the compass sensor is around 25 °C. Firstly, the microcontroller is used to get the instance temperature T_k. The variance of T_k and the desired temperature (i.e. 25 °C) would be brought to the input of a PID (proportional-integral-derivative) controller. By using a PID algorithm, the microcontroller controlled a heat/cooling generator to provide a desired temperature of the compass sensor. Note that this heat/cooling generator works based on the Peltier effect [12], and it is attached to the sensor.

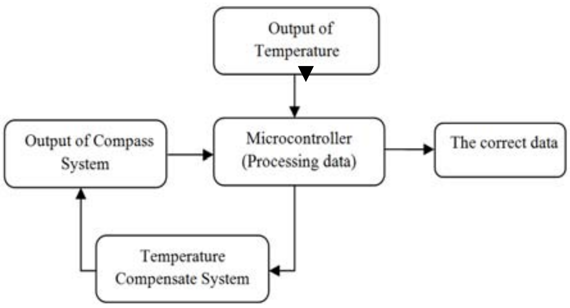

Fig. 8. Block diagram of the closed compensated compass system.

3.3. Hardware Components

The CMPS03 Digital Compass using Philips KMZ51 magnetic field sensor to determine the magnetic field of the earth, the data are processed by a microcontroller on the board (Fig. 9). This sensor is always a good choice for land or underwater navigation applications [13-14].

Fig. 9. The compass sensor CMPS03.

The temperature sensor and compass are mounted on Peltier simultaneously. This is shown in Fig. 10.

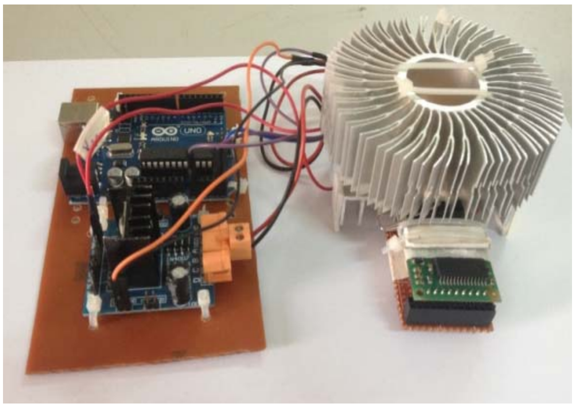

Fig. 10. The photo of the integrated system

4. Results

4.1. The Compass System is Fixed at a Position

4.1.1. The Temperature is Fixed at 25 °C

In this test, the compass sensor is fixed in a certain position of 180.3°. The data are acquired in a period of 7 minutes in order to analyze the stability of the system. The temperature is measured at 25 °C Fig. 11 shows that the sensor provides very stable values in this condition.

4.1.2. Increasing Temperature from 18 °C to 53 °C

After that, the temperature of the chamber is changed from 18 °C to 53 °C. Fig. 12(b) shows the variety of the angle values that depends on the change of the temperature (Fig. 12(a)). It is obvious that even the sensor is fixed, but the angle is changed. Thus, some solutions will be proposed in this paper to eliminate this kind of error.

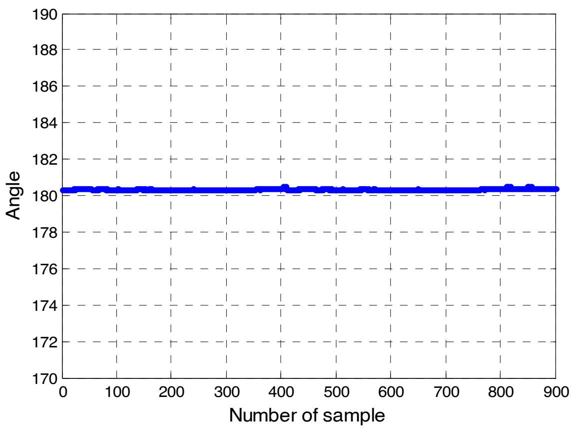

Fig. 11. Values of angle provide by the compass at the room temperature (25 °C).

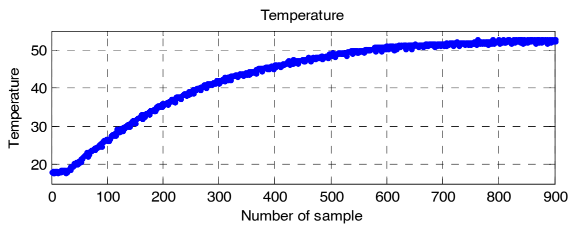

(a)

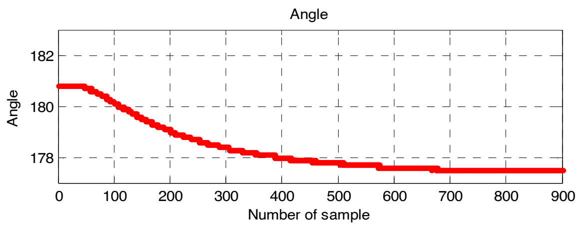

(b)

Fig. 12. Value of compass in 18-53 °C of temperature range.

For the first scheme that utilizing the feed-forward compensation, the uncompensated and feed-forward angles are in Fig. 13. It is easy to see that the feed-forward method is a good solution, even that the variation is not quite as small.

4.1.3. Decreasing Temperature from 53 °C to 18 °C

In this test, the temperature of the chamber is changed from 53 °C to 18 °C. Fig. 14 shows the comparison of the uncompensated and compensated angle outputs using feed-back structure. It can be seen that, the compensated angle output overcome the results without compensation. The variation obtained by the feed-back structure is also smaller than the variation obtained by the feed-forward structure (see Fig. 13). However, the rate of response of the Scheme 2 (i.e. feed-back structure) is slower the Scheme 1 (i.e. feed-forward structure). This is quite natural for control systems.

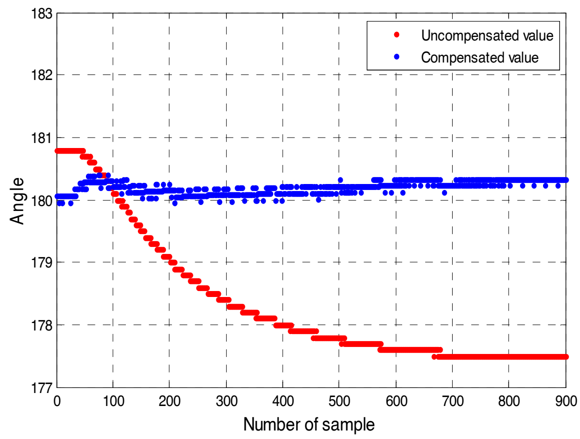

Fig. 13. Uncompensated vs. feed-forward compensated values of angles.

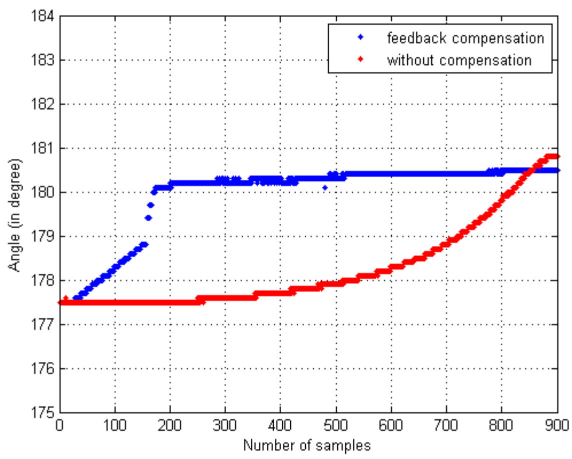

Fig. 14. Uncompensated vs. feedback compensated angles.

4.1.4. Fluctuation of the Temperature

In this test, the temperature of the chamber is fluctuated in the range of 15 °C to 25 °C as shown by the red curve in the Fig. 15(a). By using the compensated solution, the temperature is pushed back to the stable as shown by the blue curve in the Fig. 15(a). Fig. 15(b) presents the resulted angle which offer a very good stability around 180.3°.

4.1.5. Comparison between Two Schemes

In this test, the initial temperature of the sensor is 16 °C and it should reach to the designed temperature of 25 °C. Fig. 16 shows the slow response of the adjust temperature using the feed-forward structure. It takes 5 minutes to increase temperature from 16 °C to 25 °C.

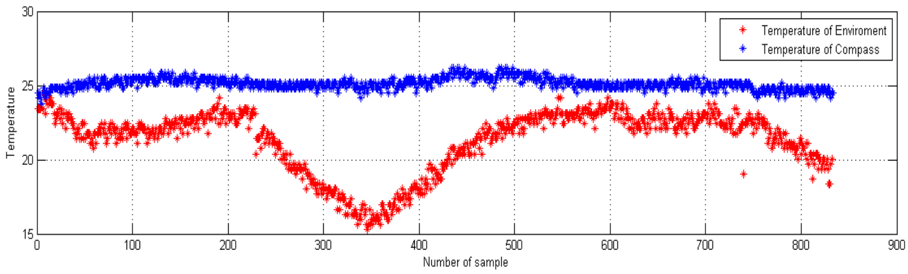

(a)

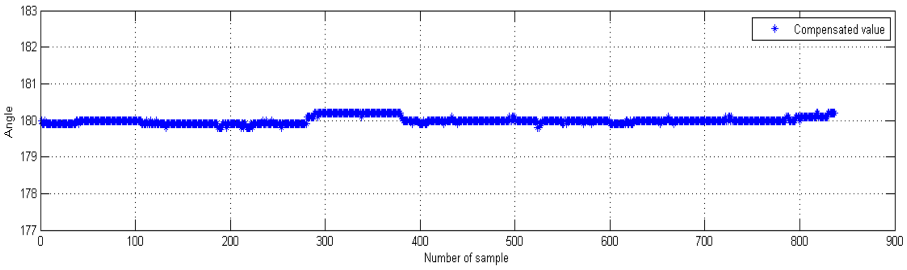

(b)

Fig. 15. Uncompensated vs. feedback compensated angles when the input temperature is fluctuating.

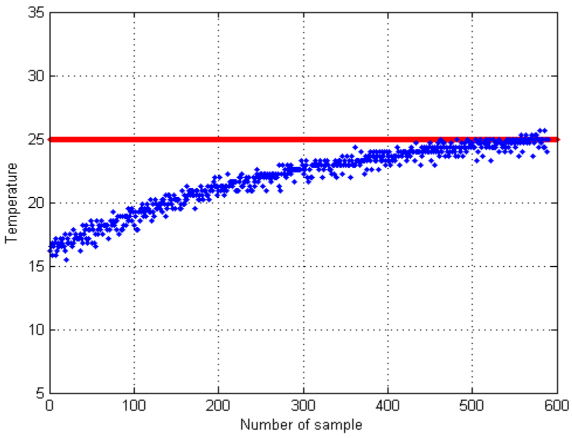

Fig. 16. Observation of temperature convergence using feed-forward compensation.

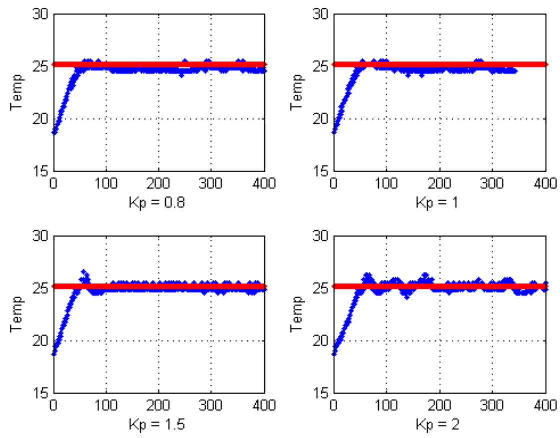

Fig. 17. The dependences of compensated outputs on the values of K_p.

In case of the feedback structure, the temperature output responses are shown in Fig. 17 with four different values of the propagation factor K_p. In this system, $K_p = 2$ offer the best response.

Fig. 18 shows the temperature output responses with four different values of the factor K_i when we keep $K_p=2$ as a good choice from previous experiment (see Fig. 17). It can be seen that, $K_i = 0.8$ provides the best response. Thus, the couples of parameter $K_p=2$, $K_i=0.8$ would be chosen for our system.

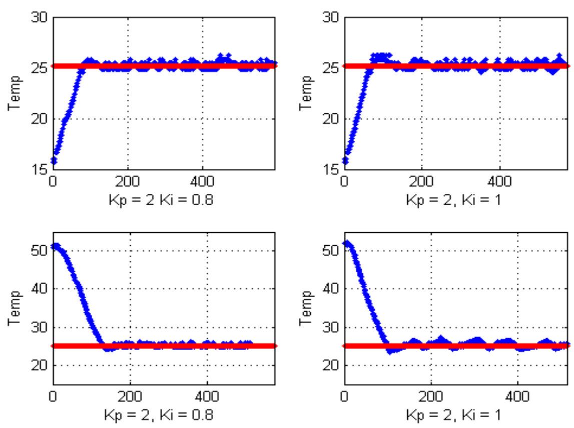

Fig. 18. The dependences of compensated outputs on the values of Kp, Ki.

4.2. The Compass System is Placed on a Turntable

4.2.1. The Temperature is Fixed at 25 °C

In this test, the temperature is fixed at 25 °C, the sensor is placed on a turntable. The turntable is rotated at speed of 0.1 rad/s. This means that it will take 7 minutes for completing one loop. It can be seen that with a stable condition of temperature, the sensor offers the angle output that very closed to the true values (see Fig. 19).

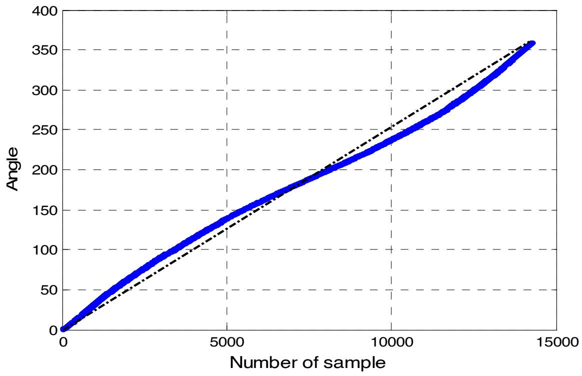

Fig. 19. The angle output of the compass sensor vs. the true angle while it was placed on a turntable at room temperature (i.e. 25 °C).

4.2.2. Fluctuation of the Temperature: Comparison between Two Schemes

Similar to the scenario in Sec. III.A.4, the temperature of the chamber is fluctuated in the range of 15 °C to 25 °C. Fig. 20 shows the compensated angle values obtained by using the feedforward and the feedback structures when the compass is placed on the turntable. As a result, the feedback structure offer a better response than the feedforward does.

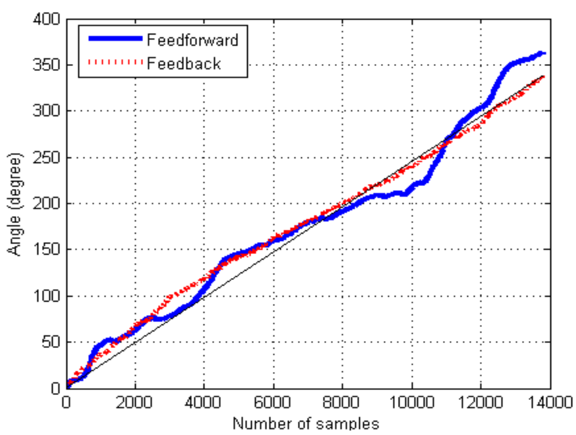

Fig. 20. The forward vs. feedback structures in compensating the angle values of the compass when it is placed on a turntable

5. Conclusions

Accuracy of the magnetic compass sensor greatly depends on the working temperature. This paper has proposed two schemes to improve the thermal stability of a specific magnetic compass sensor. These methods can be easily applied to various kinds of compass sensors. The feed-forward compensation is simple and efficient in the linear range of temperature. To extend the temperature working range of the sensor and to reduce the steady error, the feedback structure which utilizing the PID controller and the heat/cooling generator. From the experimental results, we can see that the accuracy of the magnetic compass sensor is enhanced. Obviously, this system can be applied in real applications.

References

[1]. David H. Titterton, John L. Weston, Strapdown Inertial Navigation Technology, 2nd Ed., *The American Institute of Aeronautics and Astronautics: Reston*, VA, USA, 2004.

[2]. Salytcheva A. O, Medium Accuracy INS/GPS Integration in Various GPS environments, UCGE Report Number 20200, Department of Geomatics Engineering, *University of Calgary*, September 2004.

[3]. Thang N. V., Tang P. V., Ninh V. V., Trinh C. D., Tan T. D., Application of Extended and Linear Kalman Filters for an Integrated Navigation System, in *Proceedings of the International Conference on Communications and Electronics (ICCE'12)*, Hue City, Viet Nam, 2012, pp. 574-577.

[4]. S. Godha, M. G. Petovello, G. Lachapelle, Performance Analysis of MEMS IMU/HSGPS/Magnetic Sensor Integrated System in Urban Canyons, in *Proceedings of the 18th International Technical Meeting of the Satellite Division of The Institute of Navigation (ION GNSS' 05)*, Long Beach, CA, 13-16 September 2005.

[5]. Pifu Zhang, Jason Gu, Evangelos E. Milios, Peter Huynh, Navigation with IMU/GPS/Digital Compass with Unscented Kalman Filter, in *Proceedings of the IEEE International Conference on Mechatronics & Automation*, Niagara Falls, Canada, July 2005, pp. 1497-1502.

[6]. Pavel Ripka, Improving the Accuracy of Magnetic Sensors, *Sensors*, Vol. 21, 2008, pp. 45-60.

[7]. Michael J. Caruso, Applications of magnetic sensors for low cost compass systems, in *Proceedings of the IEEE Position Location and Navigation Symposium*, 2000, pp. 177-184.

[8]. Michael J. Caruso, Applications of Magnetoresistive Sensors in Navigation Systems, *Sensors and Actuators*, SAE SP-1220, 1997, pp. 15-21.

[9]. Wei Li, Jinling Wang, Magnetic Sensors for Navigation Applications: An Overview, *The Journal of Navigation*, Vol. 67, Issue 02, 2014, pp. 263-275.

[10]. Kaveh Mohamadabadi, Anisotropic Magnetoresistance Magnetometer for inertial navigation systems, PhD Thesis, *l'Ecole Polytechnique,* 2013, pp. 30-55.

[11]. Pavel Ripka, Alois Tipek, Modern Sensors Handbook, *ISTE Ltd.*, 2007.

[12]. Magerl M., Abajian M., Krause K., Altrichter S., Siebenhaar F., Church M. K., An improved Peltier effect based instrument for critical temperature threshold measurement in cold and heat induced urticaria, *Journal of the European Academy of Dermatology and Venereology*, Vol. 29, Issue 10, 2014, pp. 2043-2045.

[13]. Le Hung P., Cuong T. D., Thinh N. T., Control for Smart Transportation Vehicle Based on Dynamic Model, Robot Intelligence Technology and Applications, *Springer Berlin Heidelberg*, 2012, pp. 993-1001.

[14]. Jaskot K., Ściegienka P., Nawrat A. M., The Prototype of an Unmanned Underwater Vehicle – Stability and Maintain a Specified Course, in Innovative Control Systems for Tracked Vehicle Platforms, *Springer International Publishing*, 2014, pp. 73-100.
